UC Davis

UC Davis Previously Published Works

Title

Preferential Destruction of Interstitial Macrophages over Alveolar Macrophages as a Cause of Pulmonary Disease in Simian Immunodeficiency Virus—Infected Rhesus Macaques

Permalink

https://escholarship.org/uc/item/41s1p8p9

Journal

The Journal of Immunology, 195(10)

ISSN

0022-1767

Authors

Cai, Yanhui

Sugimoto, Chie

Arainga, Mariluz

et al.

Publication Date

2015-11-15

DOI

10.4049/jimmunol.1501194

Peer reviewed

eScholarship.org Powered by the California Digital Library
University of California

Author Manuscript

Author Manuscript

Author Manuscript

Author Manuscript

HHS Public Access

Author manuscript

J Immunol. Author manuscript; available in PMC 2016 November 15.

Published in final edited form as:

J Immunol. 2015 November 15; 195(10): 4884–4891. doi:10.4049/jimmunol.1501194.

Preferential destruction of interstitial macrophages over alveolar macrophages as a cause of pulmonary disease in SIV-infected rhesus macaques

Yanhui Cai[*,§], **Chie Sugimoto**[*], **Mariluz Arainga**[*], **Cecily C. Mariluz**[†], **David Xianhong Liu**[†], **Xavier Alvarez**[†], **Andrew A. Lackner**[†], **Woong-Ki Kim**[¶], **Elizabeth S. Didier**[‡,‖], and **Marcelo J. Kuroda**[*,§]

[*]Divisions of Immunology, Tulane National Primate Research Center, 18703 Three Rivers Road, Covington LA 70433

[†]Comparative Pathology, Tulane National Primate Research Center, 18703 Three Rivers Road, Covington LA 70433

[‡]Microbiology, Tulane National Primate Research Center, 18703 Three Rivers Road, Covington LA 70433

[§]Department of Microbiology and Immunology, School of Medicine, Tulane University, 1430 Tulane Avenue, New Orleans, LA 70112

[¶]Department of Microbiology and Molecular Cell Biology, Eastern Virginia Medical School, Norfolk, VA 23507

[‖]Department of Tropical Medicine, School of Public Health and Tropical Medicine, Tulane University, New Orleans, LA 70112

Abstract

This study demonstrates for the first time that the AIDS virus differently impacts two distinct subsets of lung macrophages. The predominant macrophages harvested by bronchoalveolar lavage (BAL), alveolar macrophages (AM), are routinely used in studies on human lung macrophages, are long-lived cells, and exhibit low turnover. Interstitial macrophages (IM) inhabit the lung tissue, are not recovered with BAL, are shorter-lived, and exhibit higher baseline turnover rates distinct from AM. Here, we examined the effects of SIV infection on both AM in BAL and IM in lung tissue of rhesus macaques. SIV infection produced massive cell death of IM that contributed to lung tissue damage. Conversely, SIV infection induced minimal cell death of AM and these cells maintained the lower turnover rate throughout the duration of infection. This indicates that

Correspondence: Marcelo J. Kuroda, Division of Immunology, Tulane National Primate Research Center, 18703 Three Rivers Road, Covington, LA 70433; mkuroda@tulane.edu.

Author's contributions: Y.C. participated in the study design, experimental research, data analysis and manuscript preparation; C.S. participated in the research design and flow cytometry data analyses; M.A participated in studies of SIV DNA and RNA quantification study; C. Midkiff participated in SIV in situ hybridization and immunostaining studies; D.L. participated in the clinical diagnosis and interpretation of lung pathology; X. A. participated in the confocal imaging and interpretation of results; E.S.D participated in SIV pVL assay protocol development, data interpretation. and preparation of the manuscript; A.A.L and W.K kindly provided lung samples, as well as CD4+ T cell data and plasma viral load data from some of the SIV-infected monkeys, and participated in preparation of the manuscript; M.J.K participated in the study design, data interpretation, and manuscript preparation.

Author Manuscript Author Manuscript Author Manuscript Author Manuscript

SIV produces lung tissue damage through destruction of IM while the longer-lived AM may serve as a virus reservoir to facilitate HIV persistence.

Introduction

Drugs and vaccines for curing and preventing pandemic HIV/AIDS, respectively, remain elusive due to an incomplete understanding about AIDS pathogenesis. The SIV/rhesus macaque model often is used to study pathogenesis because of similarities to human HIV infections, including the loss of CD4+ T cell, general immune activation, opportunistic infections, and clinical symptoms (1). Although the decline in CD4+ T cells and/or immune activation are considered primary causes of AIDS and HIV-associated non-AIDS (HANA) morbidity and mortality, neither declining CD4+ T cells levels nor immune activation always correlate with AIDS disease progression (2). We recently reported that increased blood monocyte turnover rate predicted onset of rapid progression to AIDS and the destruction of tissue macrophages in SIV-infected rhesus macaques (2), suggesting that blood monocytes and tissue macrophages play critical roles in AIDS pathogenesis. This was consistent with, and supported by findings from Burdo and colleagues that increasing monocyte turnover rates correlated with SIV encephalitis (SIVE) progression (3) as well as our recent observation that increased monocyte turnover was associated with the accumulation of interstitial lung macrophages in SIV-infected rhesus macaques (4).

Macrophages and monocytes are primary phagocytic cells of the innate immune system and also function as major regulatory cells for tissue homeostasis and wound healing (5). Like CD4+ T cells, macrophages also are targeted by HIV and SIV that bind to surface co-receptors such as CCR5 and CCR3 (6, 7). Macrophages also play a critical role in innate immune responses to environmental exposures in the lung, and support homeostasis and resistance to respiratory infections. We recently reported that macrophages comprise ~70% of immune cells in the lungs of healthy rhesus macaques and that there are at least two major populations of lung macrophages, namely, alveolar macrophages (AM) and interstitial macrophages (IM) (8), consistent with reports about lung macrophages in humans (9). We also reported that following bronchoalveolar lavage (BAL) to harvest and remove AM, there occurred a rapid differentiation of blood monocytes and IM to putatively replace AM in the alveoli (8).

Evidence of lung pathology associated with HIV infection is observed in about 85% of AIDS lung autopsies (10), and AIDS-defining respiratory opportunistic infections (OIs) of macrophages such as pneumocystis and tuberculosis, also contribute to morbidity and mortality in HIV-infected patients (11–14). SIV replication in the BAL and lung tissue was reported as early as 7 days and 14 days after inoculation of rhesus macaques, respectively and was further confirmed within AM of the BAL by in situ hybridization (15). Microscopically, SIV-associated interstitial pneumonia has been observed as early as 2 weeks post inoculation and increased in incidence over time after inoculation (16). In addition, decreased expression of the mannose receptor, CD206, on the AM of HIV-1 infected patients correlated with defective binding and phagocytosis of *Pneumocystis jiroveci* (syn. *carinii*) (17). AM from AIDS patients also exhibited dysregulated secretion of

Author Manuscript Author Manuscript Author Manuscript Author Manuscript

the pro-inflammatory cytokine IL-12 after challenge with *Salmonella spp.* in vitro (18). These findings suggest that during HIV/SIV infection, macrophage dysfunction contributes to pathogenesis but it is still unclear how the distinct macrophage populations in the lung each contribute to HIV/AIDS or HANA conditions.

BAL can be obtained from humans to obtain AM, but IM must be recovered by lung biopsy which can be more readily accomplished in SIV-infected rhesus macaques than in HIV-infected humans (19). The purpose of this study was to use the SIV/AIDS rhesus macaque model to relate blood monocyte turnover as a measure of disease progression, with SIV infection of distinct lung macrophage populations to better understand the mechanisms of SIV-induced pulmonary pathogenesis.

Materials and methods

Animals and virus inoculations

A total of 55 adult male Indian rhesus macaques (*Macaca mulatta*) between 3.4 and 22 years of age were used in the study and housed at the Tulane National Primate Research Center in Covington, LA USA. Six monkeys served as uninfected controls. The remaining 49 monkeys were infected with 7 strains of SIV as follows: 24 monkeys received SIVmac251, 10 monkeys received SIVmac239, 3 monkeys received SIVmac239/316e*, 2 monkeys received SIVmac239ΔGY, 3 monkeys received SIVmac239ΔNef, 4 monkeys received SHIV89.6P, and 3 monkeys received SIV0302-2 (Supplemental Table S1). All of the rhesus macaques infected with SIVmac251, SIVmac239, SHIV89.6P or SIV0302-2 strains exhibited increased monocyte turnover rates during disease progression to AIDS. Animal procedures were performed according to the “NIH Guide for the Care and Use of Laboratory Animals” (National Research Council, National Academic Press, Washington, DC, 1996) and were approved by the Tulane University Institution Animal Care and Use Committee (IACUC).

BrdU/EdU injection and sample collection

The thymidine analogues, 5-bromo-2'-deoxyuridine (BrdU; Sigma Aldrich, St. Louis, MO) or 5-ethynyl-2'-deoxyuridine (EdU; Molecular Biology; Carlsbad, CA) were injected iv at 60 mg/kg or 50 mg/kg respectively. BAL samples were obtained by rinsing the lung with two aliquots of PBS (20 ml each) under a pediatric fiberoptic bronchoscope. Open chest lung biopsies of approximately 1.5 cm^3 were collected during the longitudinal studies and at necropsy, approximately 4-cm^3 sections of lung tissue were obtained for flow cytometry and (immuno)histochemistry analyses.

Isolation of macrophages and lymphocytes from lung tissue

Single-cell suspensions from lung tissues (including biopsy and necropsy samples) were prepared using enzymatic digestion. Briefly, lung tissues were sliced into 0.5 mm-thick sections after removing bronchi, and resuspended in 30 ml of RPMI1640 (Cellgro; Manassas, VA) supplemented with 5% fetal bovine serum (Gibco, cat no. 26140-079; Grand Island, NY, USA), 100 IU/ml of penicillin/streptomycin (EMD Millipore, Billerica, MA), 2 mM of L-glutamine (Cellgro; Manassas, VA), 25mM of HEPES (Molecular biology;

Author Manuscript Author Manuscript Author Manuscript Author Manuscript

Carlsbad, CA), 200 U/ml of type IV collagenase (Worthington Biochemical, cat no. 4189; Lakewood, NJ) and 0.05 mg/ml of DNase I (Roche Applied Science, cat no.10104159001; Indianapolis, IN). The suspensions were then incubated at 37°C for 30 min, followed by pipetting, incubation for an additional 10 min at 37°C, and enrichment by discontinuous density centrifugation over layers of 24% and 50% Percoll (GE Healthcare; cat no. 17-0891-01; Boston, MA) at 2000 rpm for 20 min (Beckman, Allegra X-12R, Brea, CA, USA). Cells were recovered from the 24%-50% Percoll interface, washed with 2% PBS-FBS (PBS containing 2% FBS), suspended in BAMBANKER™ serum-free cell culture freezing medium (Wako Laboratory Chemicals, cat no. 302-14681; Richmond, VA) and stored in liquid nitrogen until further analyses.

Histochemical staining of BAL cells and lung tissue

Two hundred thousand BAL cells were subjected to cytospin centrifugation (Shandon Cytospin 3, Thermo Electron Corporation) at 400 × g for 3 min, and stained with Wright-Giemsa. Differential counting was performed by light microscopy at 200× magnification. Lung pieces about 1 cm^3 collected during necropsy were processed for H&E staining. Briefly, lung tissues were fixed in 10% neutral-buffered formalin, sectioned to 6 μm thickness, stained with hematoxylin and eosin (H&E) using automated Leica autostainer XL (Leica Biosystems; Buffalo Grove, IL), and viewed under regular light microscopy at 400× magnification.

Flow cytometry

For antibody staining, 200 μl of whole blood or 10^6 cells from BAL were prepared and stained as previously reported (2). Staining for BrdU uptake was conducted using BD Pharmingen™ BrdU Flow Kit (Becton Dickinson; Cat: 559619; San Jose, USA) following surface antibody staining according to the manufacturer's protocol. EdU staining was performed using Click-iT™ EdU Pacific Blue Flow Cytometry Assay kit (Invitrogen; Cat: C-10418; Carlsbad, CA) following surface antibody staining also according to the manufacturer's protocol. A 3-laser FACSAria (Becton Dickinson; San Jose, USA) was used to detect the surface markers or intracellular BrdU/EdU incorporation in the multi-color stained cells. Antibodies used in these analyses are shown in Supplemental Table S2. AM were defined as cells expressing HLA-DR^{hi}, $CD11b^{dim}$ CD163+ CD206, and IM were defined by expressing HLA-DR+, $CD11b^{hi}$ CD163+ as previously described (8). Results were analyzed using FlowJo (Version 9.6.2, TreeStar) software.

SIV RNA in situ hybridization

To detect SIV RNA in tissues, *in situ* hybridization was performed using riboprobes as described previously (20). Briefly, 7 μm-thick formalin-fixed, paraffin-embedded tissue sections were treated sequentially with a series of xylene, ethanol and distilled water containing diethylpyrocarbonate (DEPC; Sigma; Cat: D5758; Aldrich, St. Louis, MO) for deparaffinization and rehydration before antigen retrieval. The tissue sections were blocked with saline sodium citrate (SSC) hybridization buffer containing 50% formamide with denatured herring sperm DNA and yeast tRNA at 10 mg/ml each in a humidified chamber at 45° C for 1 hr. SIV-digoxigenin-labeled anti-sense riboprobes (Lofstrands Labs Ltd;

Author Manuscript Author Manuscript Author Manuscript Author Manuscript

Gaithersburg, MD) then were applied to the tissue sections at 10 ng/slide in hybridization buffer and incubated overnight at 45° C. After hybridization, slides were washed sequentially with 2× SSC, 1× SSC, and 0.1× SSC, followed by application of blocking solution. Alkaline phosphatase-conjugated sheep anti-digoxigenin antibody diluted at 1:200 (Roche; Cat: 11093274910; Penzberg, Germany) was used to detect hybridized digoxigenin-labeled probes. The Dako cytomation Liquid Permanent Red (LPR) substrate-chromogen system (Dako, Inc. Cat: 0640; Carpinteria, CA) was prepared according to manufacturer's instructions and added to the tissue for 20 min at room temp to develop the reaction. Controls included matched positive and negative tissues hybridized with digoxigenin-labeled sense RNA-labeled probes that were processed in parallel. Rinsing with tris-buffered saline (TBS) was used to stop the reaction followed by antibody staining of the tissue sections.

Confocal microscopy imaging

Imaging was performed with a Leica TCS SP2 confocal microscope equipped with 3 lasers (Leica Microsystems) at 800× or 630× magnification and with a resolution of 512×512 pixels. Adobe Photoshop software (Version 7.0; Adobe Systems) was used to process and assemble the images. Quantification of AM and IM was performed by manually counting 20 fields of each slide at 200× final magnification.

Quantification of plasma SIV RNA and DNA in infected cells

Quantification of SIV RNA in plasma, SIV-integrated provirus, and extrachromosomal (episomal) DNA (21) in FACS-sorted cells or lung tissue was performed using the TaqMan real-time PCR method as described previously (22). SIV DNA extraction from sorted cells or lung tissue was performed using NucleoSpin® Tissue (Cat: 740952; Macherey-Nagel Inc; Bethlehem, PA) following the manufacturer's instructions. Amplification targeted a 74-bp fragment in the *gag* region and was performed in the RT-PCR Unit of the Pathogen Detection and Quantification Core at the Tulane National Primate Research Center (23). The TaqMan® RNase P Control Reagents Kit (Life Science; Cat: 4316844; Carlsbad, CA) was used to calibrate the cellular input for SIV DNA detection. All real-time PCR assays were carried out using an ABI Prism 7900HT Sequence Detection System (Applied Biosystems). Absolute viral RNA and DNA copy numbers were deduced by comparing the signal strength to corresponding values obtained from six 10-fold dilutions of standardized RNA controls that were reverse transcribed and amplified, or from standardized DNA controls that were amplified in parallel, respectively.

Statistical analysis

Comparisons between mean values were analyzed by Student *t*-test. Spearman's test was used for correlation analysis. Data were analyzed and graphed using Graphpad Prism 5 software. $P < 0.05$ was considered statistically significant.

Author Manuscript Author Manuscript Author Manuscript Author Manuscript

Results

Increased monocyte turnover correlates with severity of lung tissue damage in SIV-infected monkeys progressing to AIDS

To determine if blood monocyte turnover correlates with tissue damage in the lung, we examined lung tissue integrity in SIV-infected monkeys exhibiting different rates of blood monocyte turnover but expressing similarly low levels of circulating CD4+ T cells and high viral loads using a histological scoring system as previously described (4, 16). Microscopically, the pulmonary architecture, cellular morphology, and alveolar content in SIV-infected monkeys with low blood monocyte turnover (≤ 30%) were indistinguishable from uninfected animals. The lung tissue in these animals exhibited a thin alveolar septum lined by a single layer of flattened epithelial cells with rare macrophages in the alveoli (Fig. 1A and 1B). The pulmonary lesions associated with SIV infection were evident in the monkeys with ≥ 30% blood monocyte turnover (Fig. 1C and 1D). The alveolar septa from these animals exhibited diffuse, mild to moderate thickening characterized by increased number of mononuclear cells, capillary dilation, fibrin deposition, edema, and hyperplastic type II pneumocytes. The alveolar spaces were filled with increased numbers of foamy macrophages and multinucleated giant cells (Fig. 1C and 1D).

Increased turnover of blood monocytes in SIV-infected macaques is not reflected in the BAL

BAL specimens routinely harvested to examine innate immune responses of the lung in humans, are comprised mainly of AM but not IM (24, 25). To determine if the increased blood monocyte turnover rates that predict onset of disease progression to AIDS (2) also correlated with increased turnover of lung macrophages, we first harvested AM from BAL specimens during acute, chronic, and terminal stages of SIV infection and evaluated turnover by differential staining and flow cytometry for incorporation of BrdU/EdU. Interestingly, there was no correlation between turnover rates of AM in BAL and turnover rates of blood monocytes ($P = 0.3389$; $P = 0.7664$; $P = 0.8717$; Fig. 2A–2C). In addition, AM failed to incorporate BrdU/EdU 24 hrs (Fig. 2A), 48 hrs (Fig. 2B) or 7 days (Fig. 2C) after BrdU/EdU injection indicating that only negligible replication or replacement of AM occurred during SIV infection. Moreover, by differential cell counting, there was no significant difference in the mean percent of macrophages in BAL of SIV-infected compared to uninfected control monkeys ($P = 0.5964$; Fig. 2D). The mean absolute number of AM in BAL specimens from SIV-infected monkeys was significantly lower than from uninfected monkeys ($P = 0.0001$; Fig. 2E), but there was no correlation between blood monocyte turnover rates and BAL AM levels in SIV-infected monkeys ($P = 0.1375$; Fig. 2F).

Increased turnover rate of lung IM correlates with increased blood monocyte turnover in SIV-infected macaques

Lung tissue also was comprised a distinct subset of IM that were smaller, located exclusively in the interstitium, and phenotypically were more similar to blood monocytes than AM (8). *In vivo* BrdU labeling also demonstrated that lung IM exhibited higher baseline turnover rates similar to those of blood monocytes in uninfected macaques, unlike

Author Manuscript Author Manuscript Author Manuscript Author Manuscript

AM that exhibited very low turnover rates and thus appeared to be longer-lived (8). Thus, we compared turnover rates of lung tissue IM and blood monocytes during various stages of SIV infection, and observed that increasing blood monocyte turnover rates during disease progression to AIDS (2) also significantly correlated with increasing turnover rates of IM 24 hrs after BrdU injection (r = 0.9023; $P < 0.0001$; Fig. 3A) and 48 hrs after BrdU injection (r = 0.6434; $P < 0.0278$; Fig. 3B). Immunohistochemistry and confocal microscopy also demonstrated higher numbers of BrdU-labeled IM than AM in lung tissue of SIV-infected monkeys (Fig. 3C–3F).

Increased death rate of lung IM correlates with increased blood monocyte turnover rate in SIV-infected rhesus macaques

To determine if the increased IM turnover during SIV infection was a consequence of increased cell death, a terminal deoxynucleotidyl transferase dUTP nick-end labeling (TUNEL) technique was applied. There was a higher number of TUNEL-positive IM in lung tissues of SIV-infected animals exhibiting higher blood monocyte turnover rates than in uninfected monkeys or SIV-infected monkeys exhibiting lower blood monocyte turnover rates (Fig. 4A, 4B). Spearman's rank correlation further demonstrated statistically significant relationships between blood monocyte turnover rates and death of IM ($r = 0.9505$, $P <0.0001$; Fig. 4A), as well as with death of newly-recruited CD163+ BrdU+ TUNEL+ IM ($r = 0.5874$, $P = 0.0489$; Fig. 4B). A representative confocal microscopy image of lung tissue from an SIV-infected monkey is shown in Figure 4C

Increased SIV levels in lung tissues of infected rhesus macaques correlate with increased IM and blood monocyte turnover rates but not with SIV plasma viral loads (pVL)

To determine if SIV levels in lung macrophages correlated with death and turnover rates of IM, qPCR was used to measure SIV DNA copies in lung tissue. SIV DNA levels in the lung significantly correlated with turnover of IM represented as by the percentage of BrdU labeling at 24-hr post BrdU injection ($r = 0.6703$, $P = 0.0087$; Fig. 5A). SIV DNA levels also correlated with SIV RNA viral copies in lung tissue ($r = 0.7212$, $P < 0.0234$; Fig. 5B) suggesting active SIV replication was occurring in the lung. Interestingly, plasma viral loads (pVL) did not correlate with levels of SIV DNA and RNA in the lung (Fig. 5C). Taken together, these results suggest that the increasing virus replication destroys lung macrophages, especially IM, that may promote blood monocyte turnover for replacing the killed pulmonary macrophages.

Infection and replication of SIV in pulmonary IM and AM of rhesus macaques exhibiting high monocyte turnover

In situ hybridization of SIV RNA and confocal microscopy were performed and demonstrated that SIV infected both AM and IM in lung tissue (Fig. 6A and 6B). A higher percent of animals with monocyte turnover rates > 30% exhibited foci of SIV in both IM and AM in lung tissue while SIV foci were primarily found in IM of animals exhibiting monocyte turnover rates ≤ 30% (Supplemental Table S3). Quantitative PCR was then performed to quantify and compare SIV infection levels in AM, IM, and CD4+ T cells captured by fluorescent-activated cell sorting (FACS) of lung tissue cell suspensions (Fig.

Author Manuscript Author Manuscript Author Manuscript Author Manuscript

6C). Significantly higher levels of SIV DNA were measured in IM from animals exhibiting higher monocyte turnover rates of > 30% compared to animals exhibiting monocyte turnover rates of ≤ 30% ($P = 0.0273$; Fig. 6D). SIV DNA levels also were higher in AM of animals with higher monocyte turnover but these did not achieve a statistically significant difference compared to the mean level of SIV DNA in animals with lower monocyte turnover ($P = 0.0895$; Fig. 6D). Interestingly, SIV DNA levels in lung CD4+ T cells were similar between animals with high and low monocyte turnover rates ($P = 0.2042$; Fig. 6D). The levels of SIV RNA in plasma also did not significantly correlate with blood monocyte turnover rates ($r = -0.1193$, $P = 0.6599$; Fig. 6E). The mean number of CD4+ T cells in lungs of SIV-infected monkeys was significantly lower than in lungs of uninfected monkeys ($P < 0.0001$; Fig. 6F), but the numbers of lung CD4+ T cells in SIV-infected monkeys did not correlate with the degree of blood monocyte turnover rates indicative of disease progression ($r = -0.4818$; $P = 0.1375$ Fig. 6G).

Discussion

Results presented in an earlier publication using nonhuman primates (8) and as presented here demonstrated that there exist unique macrophage populations in the lung that display different turnover rates prior to SIV infection and different levels of SIV infection during disease progression to AIDS. HIV and SIV infect activated CD4+ T cells, but as primate lentiviruses, they also infect terminally differentiated macrophages (26–28). Declining levels of circulating CD4+ T cells are an indication of immune-deficiency, but our earlier reports demonstrated that increased turnover of circulating monocytes better predicted onset of disease progression to AIDS in SIV-infected rhesus macaques (2, 29). The results of this study further extend these finding and demonstrate that the increased levels of SIV infection and cell death of IM in lung tissue also correlated with increased blood monocyte turnover and disease progression to AIDS (2). Furthermore, the turnover rates of IM in lung tissue and blood monocytes were similar prior to infection (8) and similarly increased during SIV progression to AIDS. This suggests that the increase in blood monocyte turnover serves to replace dying SIV-infected IM in the lung. Recruitment of monocytes to replace damaged tissue macrophages has been reported during inflammation and immune responses to other infectious agents, as well (30–33). Thus, the results reported here further support a role for the newly-recruited macrophages, such as IM of the lung, in controlling infections and re-establishing tissue homeostasis (4).

The turnover of pulmonary AM, in contrast, was negligible during steady state homeostasis prior to, and during SIV infection. In addition the longer-lived AM initially were more resistant to virus infection but eventually became infected during end-stage disease, possibly via close association or contact with SIV-infected IM (Supplemental Figure. S1). The detection of BrdU-labeled AM after BAL procedure in our previous study supports the possibility that IM serve as intermediates for differentiation into AM and might transport the virus into the alveoli (8). More importantly, the increased SIV DNA in AM and IM in SIV-infected monkey exhibiting higher blood monocyte turnover strongly suggested that SIV replicated in the macrophages rather than being phagocytized for lysosomal degradation. The later infection of AM, based on detection of SIV DNA, also implied that these cells could serve as a virus reservoir (34, 35) and suggests that successful control of HIV

Author Manuscript Author Manuscript Author Manuscript Author Manuscript

infection will require elimination of virus from both T cells and macrophages (Supplemental Figure S1).

Various lineages and differentiation states of murine and humans tissue macrophages have been compared and discussed (4, 36, 37) but further in vivo characterization of human tissue macrophages is necessary for better understanding of different tissues macrophages subsets in humans. Longitudinal studies characterizing effects or shifts in mononcyte and macrophage lineages during HIV infection in humans are difficult to accomplish so studies using nonhuman primates are expected to provide basic information to guide such investigations. This study demonstrated that SIV affects at least two subsets of lung macrophages differently, and strongly suggests that there exist functional differences between the shorter-lived IM and longer-lived AM of the lung. The direct link between the turnover of circulating monocytes and destruction of IM, but not AM of the lung further supports a role for IM in homeostasis and/or the daily protection of the lung (4). Although not addressed in the present study, it will be important to understand the molecular mechanisms for SIV-induced cell killing of IM but not of AM in the lung tissues to include measurement for determining the level of cell death factors or cell survival factors (e.g. hexokinase-6) in different macrophage subsets as previously described (38).

Studies on lung biology and innate immunity in humans typically rely on the use of BAL specimens. A limitation is that BAL specimens are comprised almost exclusively of AM but not IM. Evidence of viral infection of AM, pneumonia, opportunistic infection or neoplasms is observed both in humans and macaques (39) while the impact of HIV-1 infection of IM in humans has been under-examined. AM and IM of the lung exhibit different kinetics in turnover and SIV infection rates, suggesting that BAL samples may provide an incomplete or limited representation of pulmonary immune responses. Therefore, a reliable and accessible marker of lung tissue damage produced by HIV/SIV infection, IM damage and higher monocyte turnover is expected to monitor lung pathogenesis longitudinally during progression to AIDS, and perhaps also for development of HANA conditions. It is important to note that the pathology of the lung observed in the SIV-infected macaques described in this study (Fig. 1) may somewhat differ from the lesions generally described in lung tissue of HIV-infected humans. This is mainly because lung tissue specimens collected in our study were based on an experimental timeline to relate blood monocyte turnover rate to lung tissue changes at time points that also were prior to clinical signs of pneumonia or development of opportunistic infections. Lung tissues from HIV-infected humans were primarily obtained for purposes of diagnostics and treatment only after clinical signs, such as pneumonia arose, or from autopsy tissue to help determine cause of death. However, lung tissue of SIV-infected macaques obtained at the late stage with pneumonia produced similar lung lesions as previously reported from HIV-infected humans (16, 40, 41). Although, more detailed studies are necessary and are underway, some candidate biomarkers of increasing monocyte turnover coincident to disease pathogenesis may include neopterine, IP10 and sCD163 (data not sown). In addition, plasma CXCL13 could also be considered since it has been reported to correlate with the level of plasma viral load in HIV-infected cohorts (42), although our study indicated that not all SIV-infected macaques with high viral load exhibited high monocyte turnover, so this is another area of exploration. Patro et al. (43) reported that apoptosis of monocytes correlated with HIV plasma levels and while SIV

Author Manuscript Author Manuscript Author Manuscript Author Manuscript

levels did not necessarily correlate with disease progression in our studies using rhesus macaques, monocyte apoptosis could also be considered for its relationship or impact on monocyte turnover. The nonhuman primate model of AIDS is especially amenable to examining these mechanisms and their impact on both populations of lung macrophages via BAL and tissue biopsy and thus provides an important resource for studies about the mechanisms of HIV/AIDS and HANA pathogenesis as well as for defining sites of viral reservoirs necessary to rationally target effective therapies.

Supplementary Material

Refer to Web version on PubMed Central for supplementary material.

Acknowledgments

We thank Toni P. Penny, Desiree K Waguespack, Ashley N. Leach, Erin M. Haupt, Julie Bruhn and Calvin Lanclos in the Division of Immunology, Chris Monjure and Coty Tatum in the Pathogen Detection and Quantification Core of the Division of Microbiology, and Dr. Jason P. Dufour in the Division of Veterinary Medicine at TNPRC for technical assistance.

Financial Support:

This study was supported by grants from the National Institutes of Health to MJK (AI097059, AI087302, AI091501 and AI110163) and to the Tulane National Primate Research Center (OD011104) and a grant from Virginia's Commonwealth Health Research Board to W.K.K (#11-09).

References

1. Van Rompay KK. The use of nonhuman primate models of HIV infection for the evaluation of antiviral strategies. AIDS research and human retroviruses. 2012; 28:16–35. [PubMed: 21902451]
2. Hasegawa A, Liu H, Ling B, Borda JT, Alvarez X, Sugimoto C, Vinet-Oliphant H, Kim WK, Williams KC, Ribeiro RM, Lackner AA, Veazey RS, Kuroda MJ. The level of monocyte turnover predicts disease progression in the macaque model of AIDS. Blood. 2009; 114:2917–2925. [PubMed: 19383966]
3. Burdo TH, Soulas C, Orzechowski K, Button J, Krishnan A, Sugimoto C, Alvarez X, Kuroda MJ, Williams KC. Increased monocyte turnover from bone marrow correlates with severity of SIV encephalitis and CD163 levels in plasma. PLoS pathogens. 2010; 6:e1000842. [PubMed: 20419144]
4. Cai Y, Sugimoto C, Liu DX, Midkiff CC, Alvarez X, Lackner AA, Kim WK, Didier ES, Kuroda MJ. Increased monocyte turnover is associated with interstitial macrophage accumulation and pulmonary tissue damage in SIV-infected rhesus macaques. Journal of leukocyte biology. 2015; 97:1147–1153. [PubMed: 25780057]
5. Lin SL, Castano AP, Nowlin BT, Lupher ML Jr, Duffield JS. Bone marrow Ly6Chigh monocytes are selectively recruited to injured kidney and differentiate into functionally distinct populations. J Immunol. 2009; 183:6733–6743. [PubMed: 19864592]
6. He J, Chen Y, Farzan M, Choe H, Ohagen A, Gartner S, Busciglio J, Yang X, Hofmann W, Newman W, Mackay CR, Sodroski J, Gabuzda D. CCR3 and CCR5 are co-receptors for HIV-1 infection of microglia. Nature. 1997; 385:645–649. [PubMed: 9024664]
7. Lai J, Bernhard OK, Turville SG, Harman AN, Wilkinson J, Cunningham AL. Oligomerization of the macrophage mannose receptor enhances gp120-mediated binding of HIV-1. The Journal of biological chemistry. 2009; 284:11027–11038. [PubMed: 19224860]
8. Cai Y, Sugimoto C, Arainga M, Alvarez X, Didier ES, Kuroda MJ. In vivo characterization of alveolar and interstitial lung macrophages in rhesus macaques: implications for understanding lung disease in humans. J Immunol. 2014; 192:2821–2829. [PubMed: 24534529]
9. Misharin AV, Scott Budinger GR, Perlman H. The lung macrophage: a Jack of all trades. American journal of respiratory and critical care medicine. 2011; 184:497–498. [PubMed: 21885631]

Author Manuscript Author Manuscript Author Manuscript Author Manuscript

10. Li H, Singh S, Gorantla S, Potula R, Persidsky Y, Poluektova L, Kanmogne GD. Dysregulation of Claudin-5 in HIV-induced Interstitial Pneumonitis and Lung Vascular Injury: Protective Role of PPAR-gamma. American journal of respiratory and critical care medicine. 2012
11. Huang L, Cattamanchi A, Davis JL, den Boon S, Kovacs J, Meshnick S, Miller RF, Walzer PD, Worodria W, Masur H. H. I. V. a. O. P. S. International, and H. I. V. S. Lung. HIV-associated Pneumocystis pneumonia. Proceedings of the American Thoracic Society. 2011; 8:294–300. [PubMed: 21653531]
12. Pawlowski A, Jansson M, Skold M, Rottenberg ME, Kallenius G. Tuberculosis and HIV co-infection. PLoS pathogens. 2012; 8:e1002464. [PubMed: 22363214]
13. Morris A, Lundgren JD, Masur H, Walzer PD, Hanson DL, Frederick T, Huang L, Beard CB, Kaplan JE. Current epidemiology of Pneumocystis pneumonia. Emerging infectious diseases. 2004; 10:1713–1720. [PubMed: 15504255]
14. Lian YL, Heng BS, Nissapatorn V, Lee C. AIDS-defining illnesses: a comparison between before and after commencement of highly active antiretroviral therapy (HAART). Current HIV research. 2007; 5:484–489. [PubMed: 17896968]
15. Barber SA, Gama L, Li M, Voelker T, Anderson JE, Zink MC, Tarwater PM, Carruth LM, Clements JE. Longitudinal analysis of simian immunodeficiency virus (SIV) replication in the lungs: compartmentalized regulation of SIV. The Journal of infectious diseases. 2006; 194:931–938. [PubMed: 16960781]
16. Baskin GB, Murphey-Corb M, Martin LN, Soike KF, Hu FS, Kuebler D. Lentivirus-induced pulmonary lesions in rhesus monkeys (Macaca mulatta) infected with simian immunodeficiency virus. Vet Pathol. 1991; 28:506–513. [PubMed: 1771740]
17. Koziel H, Eichbaum Q, Kruskal BA, Pinkston P, Rogers RA, Armstrong MY, Richards FF, Rose RM, Ezekowitz RA. Reduced binding and phagocytosis of Pneumocystis carinii by alveolar macrophages from persons infected with HIV-1 correlates with mannose receptor downregulation. The Journal of clinical investigation. 1998; 102:1332–1344. [PubMed: 9769325]
18. Gordon MA, Gordon SB, Musaya L, Zijlstra EE, Molyneux ME, Read RC. Primary macrophages from HIV-infected adults show dysregulated cytokine responses to Salmonella, but normal internalization and killing. AIDS. 2007; 21:2399–2408. [PubMed: 18025876]
19. Picinin IF, Camargos PA, Marguet C. Cell profile of BAL fluid in children and adolescents with and without lung disease. Jornal brasileiro de pneumologia : publicacao oficial da Sociedade Brasileira de Pneumologia e Tisilogia. 2010; 36:372–385. [PubMed: 20625676]
20. Borda JT, Alvarez X, Kondova I, Aye P, Simon MA, Desrosiers RC, Lackner AA. Cell tropism of simian immunodeficiency virus in culture is not predictive of in vivo tropism or pathogenesis. The American journal of pathology. 2004; 165:2111–2122. [PubMed: 15579453]
21. Buzon MJ, Codoner FM, Frost SD, Pou C, Puertas MC, Massanella M, Dalmau J, Llibre JM, Stevenson M, Blanco J, Clotet B, Paredes R, Martinez-Picado J. Deep molecular characterization of HIV-1 dynamics under suppressive HAART. PLoS pathogens. 2011; 7:e1002314. [PubMed: 22046128]
22. Gautam R, Gaufin T, Butler I, Gautam A, Barnes M, Mandell D, Pattison M, Tatum C, Macfarland J, Monjure C, Marx PA, Pandrea I, Apetrei C. Simian immunodeficiency virus SIVrcm, a unique CCR2-tropic virus, selectively depletes memory CD4+ T cells in pigtailed macaques through expanded coreceptor usage in vivo. Journal of virology. 2009; 83:7894–7908. [PubMed: 19493994]
23. Monjure CJ, Tatum CD, Panganiban AT, Arainga M, Traina-Dorge V, Marx PA Jr, Didier ES. Optimization of PCR for quantification of simian immunodeficiency virus genomic RNA in plasma of rhesus macaques (Macaca mulatta) using armored RNA. Journal of medical primatology. 2014; 43:31–43. [PubMed: 24266615]
24. Ieong MH, Reardon CC, Levitz SM, Kornfeld H. Human immunodeficiency virus type 1 infection of alveolar macrophages impairs their innate fungicidal activity. American journal of respiratory and critical care medicine. 2000; 162:966–970. [PubMed: 10988114]
25. Guth AM, Janssen WJ, Bosio CM, Crouch EC, Henson PM, Dow SW. Lung environment determines unique phenotype of alveolar macrophages. American journal of physiology. Lung cellular and molecular physiology. 2009; 296:L936–L946. [PubMed: 19304907]

Author Manuscript Author Manuscript Author Manuscript Author Manuscript

26. Freed EO, Martin MA. HIV-1 infection of non-dividing cells. Nature. 1994; 369:107–108. [PubMed: 8192816]
27. Aggarwal A, McAllery S, Turville SG. Revising the Role of Myeloid cells in HIV Pathogenesis. Current HIV/AIDS reports. 2013; 10:3–11. [PubMed: 23242701]
28. Ayinde D, Maudet C, Transy C, Margottin-Goguet F. Limelight on two HIV/SIV accessory proteins in macrophage infection: is Vpx overshadowing Vpr? Retrovirology. 2010; 7:35. [PubMed: 20380700]
29. Kuroda MJ. Macrophages: do they impact AIDS progression more than CD4 T cells? Journal of leukocyte biology. 2010; 87:569–573. [PubMed: 20053708]
30. Murray PJ, Wynn TA. Protective and pathogenic functions of macrophage subsets. Nature reviews. Immunology. 2011; 11:723–737.
31. Shi C, Pamer EG. Monocyte recruitment during infection and inflammation. Nature reviews. Immunology. 2011; 11:762–774.
32. Fangradt M, Hahne M, Gaber T, Strehl C, Rauch R, Hoff P, Lohning M, Burmester GR, Buttgereit F. Human monocytes and macrophages differ in their mechanisms of adaptation to hypoxia. Arthritis research & therapy. 2012; 14:R181. [PubMed: 22870988]
33. Westhorpe CL, Zhou J, Webster NL, Kalionis B, Lewin SR, Jaworowski A, Muller WA, Crowe SM. Effects of HIV-1 infection in vitro on transendothelial migration by monocytes and monocyte-derived macrophages. Journal of leukocyte biology. 2009; 85:1027–1035. [PubMed: 19286896]
34. Swanstrom R, Coffin J. HIV-1 pathogenesis: the virus. Cold Spring Harbor perspectives in medicine. 2012; 2:a007443. doi007410.001101/cshperspect.a007443. [PubMed: 23143844]
35. Koppensteiner H, Brack-Werner R, Schindler M. Macrophages and their relevance in Human Immunodeficiency Virus Type I infection. Retrovirology. 2012; 9:82. [PubMed: 23035819]
36. Haniffa M, Bigley V, Collin M. Human mononuclear phagocyte system reunited. Semin Cell Dev Biol. 2015; 41:59–69. [PubMed: 25986054]
37. Davies LC, Taylor PR. Tissue-resident macrophages: then and now. Immunology. 2015; 144:541–548. [PubMed: 25684236]
38. Sen S, Kaminiski R, Deshmane S, Langford D, Khalili K, Amini S, Datta PK. Role of hexokinase-1 in the survival of HIV-1-infected macrophages. Cell cycle. 2015; 14:980–989. [PubMed: 25602755]
39. Beck JM, Rosen MJ, Peavy HH. Pulmonary complications of HIV infection. Report of the Fourth NHLBI Workshop. American journal of respiratory and critical care medicine. 2001; 164:2120–2126. [PubMed: 11739145]
40. Martin LN, Murphey-Corb M, Soike KF, Davison-Fairburn B, Baskin GB. Effects of initiation of 3'-azido,3'-deoxythymidine (zidovudine) treatment at different times after infection of rhesus monkeys with simian immunodeficiency virus. J Infect Dis. 1993; 168:825–835. [PubMed: 7690823]
41. Sui Y, Li S, Pinson D, Adany I, Li Z, Villinger F, Narayan O, Buch S. Simian human immunodeficiency virus-associated pneumonia correlates with increased expression of MCP-1, CXCL10, and viral RNA in the lungs of rhesus macaques. Am J Pathol. 2005; 166:355–365. [PubMed: 15681820]
42. Cohen KW, Dugast AS, Alter G, McElrath MJ, Stamatatos L. HIV-1 single-stranded RNA induces CXCL13 secretion in human monocytes via TLR7 activation and plasmacytoid dendritic cell-derived type I IFN. J Immunol. 2015; 194:2769–2775. [PubMed: 25667414]
43. Patro SC, Pal S, Bi Y, Lynn K, Mounzer KC, Kostman JR, Davuluri RV, Montaner LJ. Shift in monocyte apoptosis with increasing viral load and change in apoptosis-related ISG/Bcl2 family gene expression in chronically HIV-1-infected subjects. Journal of virology. 2015; 89:799–810. [PubMed: 25355877]

Author Manuscript
Author Manuscript
Author Manuscript
Author Manuscript

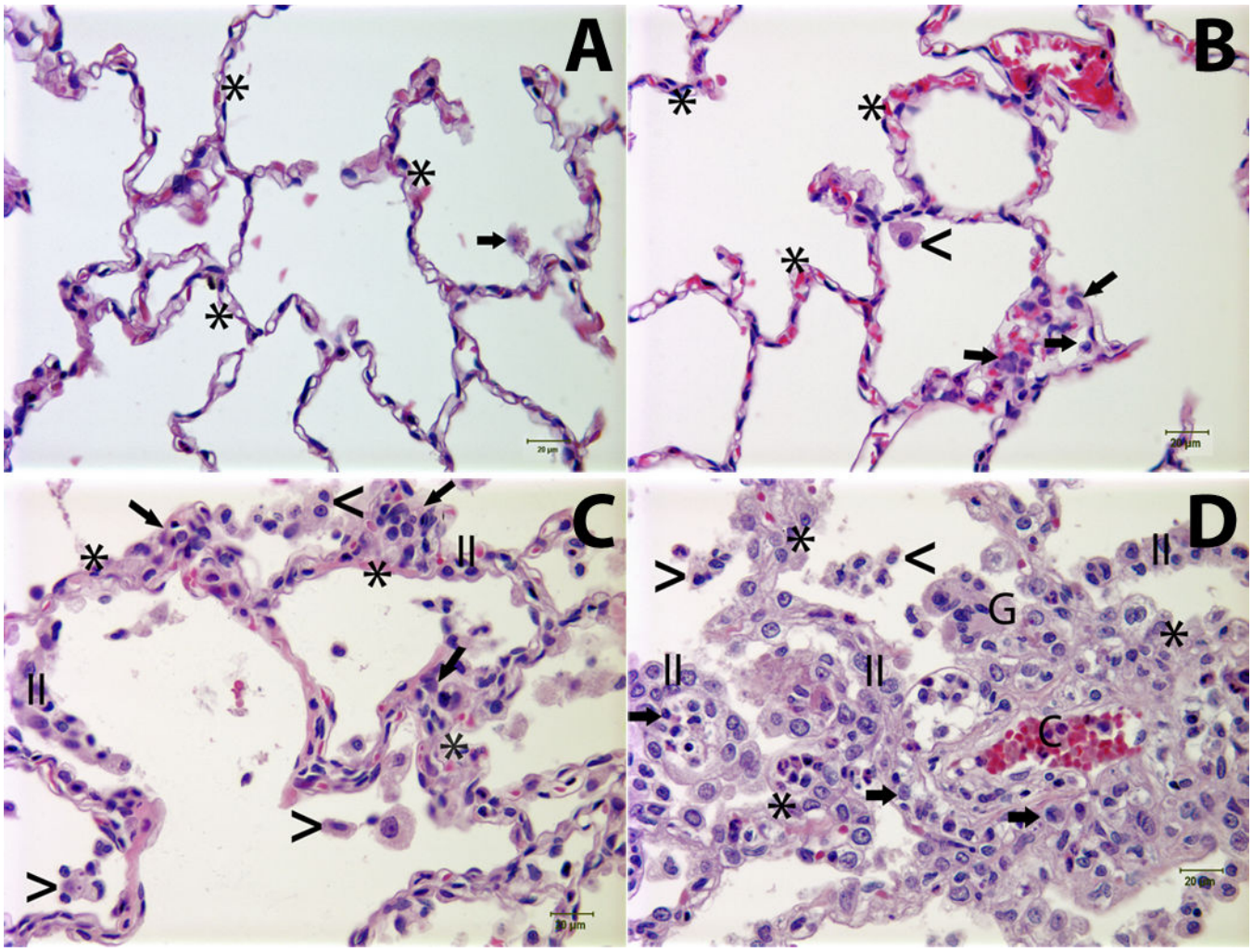

Figure 1. The severity of pulmonary lesions correlated with the rate of monocyte turnover (RMT) in SIV-infected rhesus macaques

Panel A: Normal lung tissue from an uninfected monkey [the rate of monocyte turnover (RMT) = 1.61%]; **Panel B**: Lung tissue from an SIV-infected animal (RMT = 22.7%) demonstrates minimal interstitial accumulation of a few mononuclear cells (arrows) and rare alveolar macrophages (<); **Panels C and D**: Lung tissues from SIV-infected animals with RMT = 40.5% and RMT= 55%, respectively, exhibited mild (**Panel C**) to moderate (**Panel D**) interstitial pneumonia characterized by alveolar septa thickening, capillary dilation (C), increased the numbers of mononuclear cells (arrows) and hyperplastic type II pneumocytes (II). Low (**Panel C**) to moderate (**Panel D**) numbers of alveolar macrophages (<) and multinucleated giant cells (G) were noted in the alveolar spaces. Asterisk (*) = alveolar septum. Tissues were stained with H&E and viewed at 400× magnification. Lung injury was assessed using a histological scoring system as previously described (4, 16).

Author Manuscript Author Manuscript Author Manuscript Author Manuscript

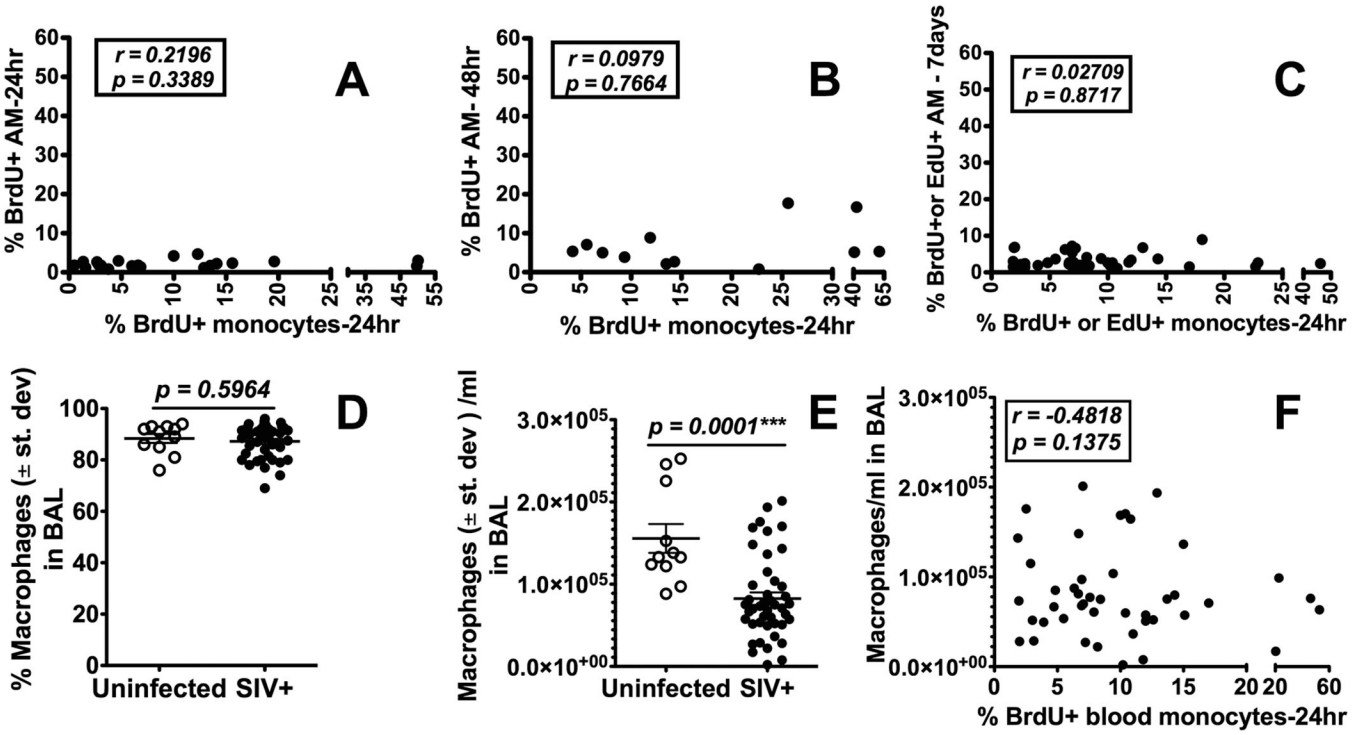

Figure 2. Increased turnover of blood monocytes in SIV-infected macaques is not reflected in the BAL

BAL samples were collected prior to and during different stages of SIV infection from rhesus macaques. BrdU or EdU was injected i.v. into SIV-infected rhesus macaques and the turnover of blood monocytes and AM recovered from BAL was analyzed by flow cytometry. There was no statistically significant correlation between blood monocyte turnover and AM turnover at 24 hr after BrdU/EdU injection (**A**: n= 21), 48 hr (**B**: n=12) and 7 days later (**C**: n=38) using Spearman's correlation analysis. There also was no difference in the percent of macrophages recovered in BAL from SIV-infected vs uninfected macaques (**D**) although there was a significant decrease in the absolute number of macrophages recovered from BAL of SIV-infected compared to uninfected macaques by Student's *t* test (**E**). The numbers of macrophages recovered from BAL of SIV-infected monkeys did not correlate with blood monocyte turnover by Spearman's correlation analysis (**F**).

Author Manuscript Author Manuscript Author Manuscript Author Manuscript

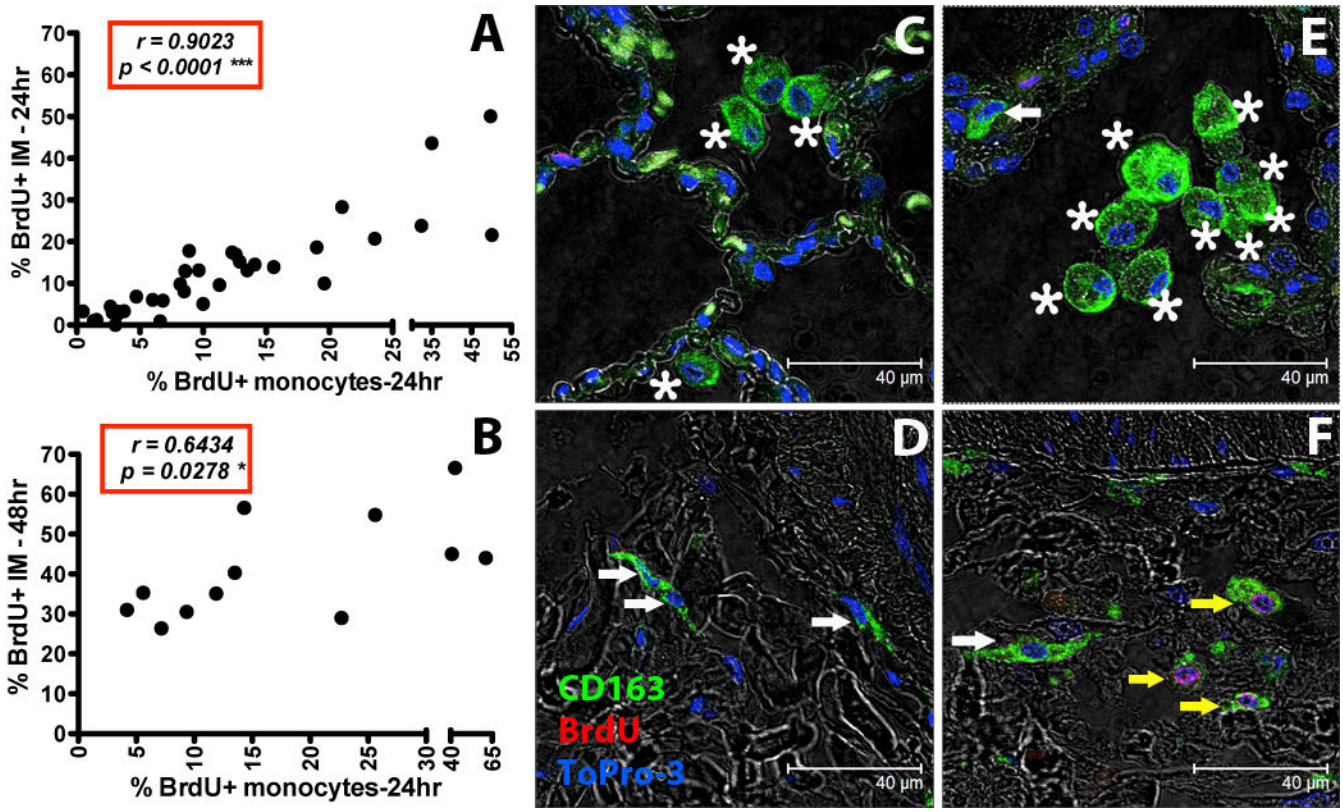

Figure 3. Increased turnover rate of lung IM correlates with increased blood monocyte turnover in SIV-infected macaques

BrdU or EdU was injected i.v. into SIV-infected or uninfected rhesus macaques and lung IM were analyzed by flow cytometry (**A** and **B**). By Spearman's correlation analyses, a significant correlation was observed between blood monocyte turnover and IM turnover 24 hr (**A**: n = 35) or 48hr (**B**: n = 12) after BrdU/EdU injection. Paraffin-embedded lung tissue sections obtained after necropsy from uninfected (**C** and **D**: representative of 4 animals) and SIV-infected rhesus macaques (**E** and **F**: representative of 4 animals) were stained with anti-CD163 antibody (macrophages-Green), anti-BrdU antibody (turnover-Red) and Topro-3 (nucleic acid-Blue). Images were captured with a Leica TCS SP2 confocal microscope equipped with a 3-laser (Leica Microsystems) under an oil objective (63×, fluotar/NA 1.0) for a final magnification of 1260×. White arrows indicate CD163-staining IM cells (green), yellow arrows indicate CD163-staining IM cells that incorporated BrdU (green and red), and asterisks indicate CD163-staining AM (green).

Author Manuscript Author Manuscript Author Manuscript Author Manuscript

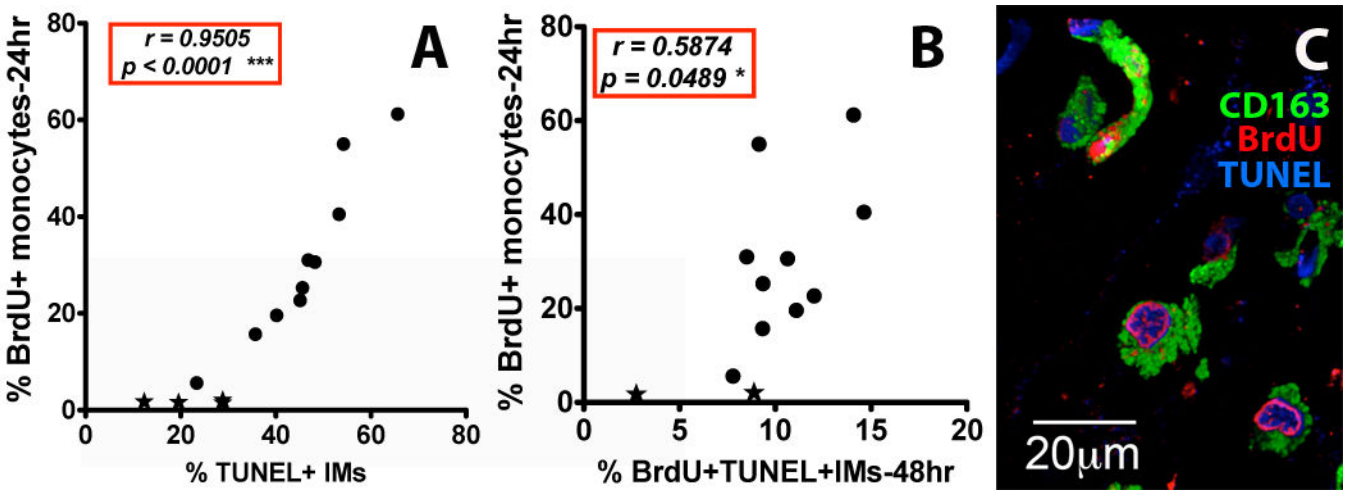

Figure 4. Increased death rate of lung IM correlates with increased blood monocyte turnover rate in SIV-infected rhesus macaques

(**A**) Spearman's correlation analyses were performed to relate blood monocyte turnover (BrdU) and percent of TUNEL+ IM (cell death) from lungs of uninfected and SIV-infected monkeys collected 24 hr post BrdU injection (n=14), and (**B**) 48 hr post BrdU injection (n=12). A minimum of 400 cells were counted in at least 5 microscopic fields of lung tissues from SIV-infected (●) and uninfected (★) monkeys. (**C**) A representative image of IM in the lung tissues from an SIV-infected monkey with high monocyte turnover (55% BrdU-staining monocytes at 24h) is shown. Lung tissues from four uninfected rhesus macaques and ten SIV-infected monkeys with different monocyte turnover rates were stained with anti-CD163 (Green) and anti-BrdU (turnover-Red) antibodies. Cell death/apoptosis was measured by TUNEL (Blue) staining. Images were captured with a Leica TCS SP2 confocal microscope at a final magnification of 1260×.

Author Manuscript Author Manuscript Author Manuscript Author Manuscript

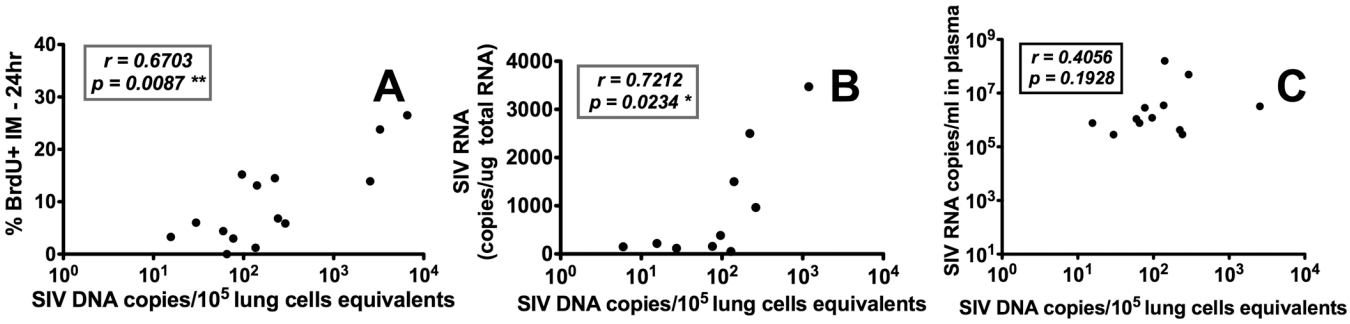

Figure 5. Increased SIV levels in lung tissues of infected rhesus macaques correlate with increased IM and blood monocyte turnover rates but not with SIV plasma viral loads (pVL)

Lung tissues were collected from SIV-infected macaques at different stages of disease and quantitated for SIV DNA and RNA. (**A**) The number of SIV DNA copy equivalents in lung tissue directly correlated with IM turnover in SIV-infected macaques (n=14). (**B**) SIV DNA copy numbers directly correlated with SIV RNA copy numbers in the lungs of SIV-infected macaques (n=10). (**C**) SIV DNA copy numbers in lung did not correlate with the pVL in SIV-infected macaques (n=12). Spearman's correlation analyses were applied for statistical analysis.

Author Manuscript Author Manuscript Author Manuscript Author Manuscript

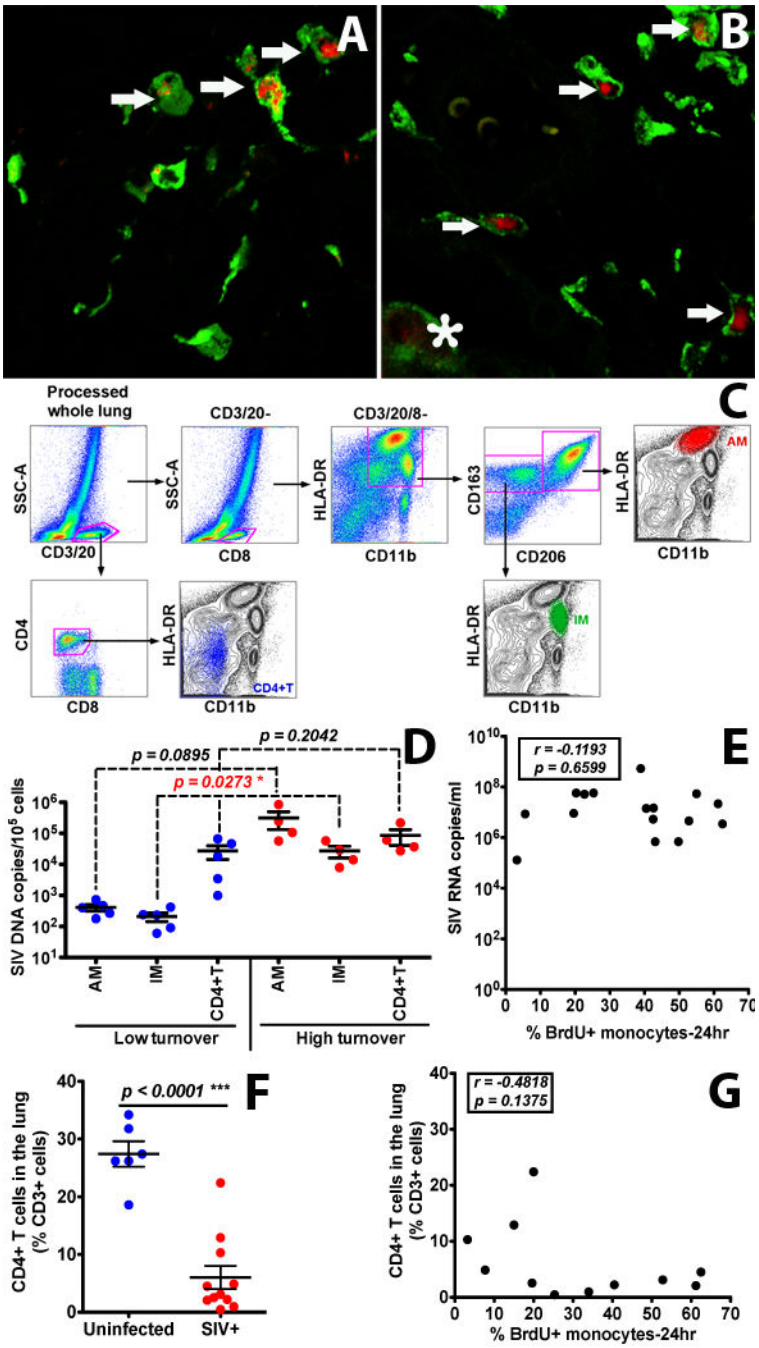

Figure 6. Infection and replication of SIV in IM and AM contribute to the viral load in lung tissues of infected rhesus macaques exhibiting high monocyte turnover

(**A&B**) Confocal microscopy was performed on lung tissues obtained from SIV-infected monkeys with low (≤ 30%) monocyte turnover (**A**: n=3) and higher (> 30%) blood monocyte turnover levels (**B**: n=6). Anti-CD163 (Green) antibody was used to identify macrophages, and SIV RNA (Red) was detected with anti-sense riboprobes. Arrows indicate SIV-infected IM. The asterisk indicates an SIV-infected AM. (**C**) Gating strategy for analyzing and sorting AM, IM and CD4+ T cells isolated from lung tissue. (**D**) IM, AM and

Author Manuscript Author Manuscript Author Manuscript Author Manuscript

CD4+ T cells were sorted via FACS from single-cell suspensions of lung tissues from SIV-infected monkeys with low (n=5) and high (n=4) blood monocyte turnover, and SIV DNA levels were quantitated and standardized against RNase P levels. (**E**) Plasma VL did not correlate with monocyte turnover in SIV-infected macaques. (**F**) CD4+ T cell depletion in the lung of all SIV-infected macaques was evident ($p<0.0001$). (**G**) The levels of CD4+ T cells did not correlate with monocyte turnover rates in SIV-infected macaques. Student's *t* test was applied for comparisons in results shown in **panels D** and **F**, and Spearman's correlation analysis was applied in results shown in **panels E** and **G**.